NUMERICAL SIMULATION AND CIRCUIT NETWORK MODELLING OF FLOW DISTRIBUTIONS IN 2-D ARRAY CONFIGURATIONS

by

Jingyu WANG, Jian YANG, Long LI, Pei QIAN, and Qiuwang WANG[*]

Key Laboratory of Thermo-Fluid Science and Engineering, Ministry of Education,
Xi'an Jiaotong University, Xi'an, Shaanxi, China

Packing configuration is widely used in chemical industries such as chemical reaction and chromatograph where the flow distribution has a significant effect on the performance of heat and mass transfer. In the present paper, numerical simulation is carried out to investigate the fluid-flow in three 2-D array configurations including in-line array, staggered array and hexagonal array. Meanwhile, a simplified equivalent circuit network model based on the Voronoi tessellation is proposed to simulate the flow models. It is found that firstly, the local Reynolds number could be used as a criterion to determine the flow regime. Flow with maximum local Reynolds number less than 40 could be regarded as Darcy flow. Secondly, the flow pattern can be well represented by the network model in the range of Darcy flow with the determination method of hydraulic resistance proposed in the present paper.

Key words: *voronoi tessellation (diagram), equivalent circuit model,*
electrical-fluidic analogy, darcy flow, flow pattern

Introduction

Packing configurations are common elements which are widely used in real applications such as chemical packed bed reactor [1], chromatographic separation [2], and heat sinks [3]. Yang *et al.* [1] revealed that structured packed beds have different flow and heat transfer characteristics compared with randomly packed beds. Li *et al.* [2] found different packing structures such as simple cubic packing, body-centered cubic packing, and face-centered cubic packing may lead to various flow patterns and mass transfer performances in chromatography separation. The pressure drop and cooling performance of heat sinks with different shaped pin-fin structures arranged in staggered and in-line order were studied by Arjun and Kumar [3]. Sayehvand *et al.* [4] studied the forced convective heat transfer over three cylinders in staggered arrangement. Wang *et al.* [5] changed the structure of the packing configuration and an obvious improvement on the heat transfer performance was obtained. From the previouses study, we could find the packing configuration has a significant effect on the flow field and thus influence the whole pressure drop and heat and mass transfer performance.

The flow field in packing configurations could be obtained either by experimental investigation or numerical simulation. In terms of experiment, particle image velocimetry

---

[*] Corresponding author; e-mail: wangqw@mail.xjtu.edu.cn

1988

Wang, J., *et al.*: Numerical Simulation and Circuit Network Modelling…
THERMAL SCIENCE: Year 2018, Vol. 22, No. 5, pp. 1987-1998

(PIV) technique [6] and magnetic resonance imaging (MRI) technique [7] have been used to obtain the local velocity in the pores. On the other hand, the transport phenomenon in randomly packed bed with raschig rings was numerically studied by Marek [8], while packed bed with spherical particles was simulated by Dae *et al.* [9]. However, experiments measuring the flow fields are expensive and the numerical simulation is demanding for computer resources. Therefore, the motivation of the present work is to find the relationship between the flow field and packing configuration in order to acquire the flow pattern of a certain configuration quickly.

There are some parameters to evaluate the configuration of packed bed, such as the porosity, radial and axial porosity distribution, the co-ordination number, the radial distribution function, the angle distribution function, the Voronoi tessellation and so on [10]. Among these parameters, the Voronoi tessellation of packed bed refers to the division of region. The Voronoi cell (or Voronoi polygon) of a particle is delimited by the smallest envelope of bisecting lines with the other particles [11]. The edges in 2-D Voronoi tessellation and faces in 3-D Voronoi tessellation correspond to the porosity between particles where the fluid may pass. So the relationship between the Voronoi tessellation of packed beds and their flow paths is expected.

The Voronoi tessellation has been used to investigate the conduction and radiation in packed bed [12] since it could represent the contact model among the particles. Chareyre and Cortis [13] carried out a pore-scale modelling based on the Voronoi tessellation in dense sphere packings to study the effective permeability and forces induced on the particles.

In the present study, we are going to build a circuit network model based on the Voronoi tessellation to study whether this model could be used to predict the flow distributions in packing configurations quickly compared with numerical simulation. Actually, the network modelling in porous media has been widely used. Koplik [14] and Chu and Ng [15] investigated the permeability in porous media by a network model. However, these network models just focused on the whole characteristics such as permeability, where the relationship between the local flow rate and structure parameter could not be obtained. There are also some other studies using the real topological and geometrical properties to build the pore network of packed beds in single phase flow [16] and gas-liquid two phases flow [17]. However, the structural reconstruction by X-ray micro-tomography is money and time consuming. Besides, the channel conductivity has an influence on the accuracy of the results and thus still needs to be further studied.

In the present paper, the fluid flow in 2-D array configurations with circular shape is investigated. Numerical simulation performed by ANSYS FLUENT R16.0 is used to study the flow regimes as well as to verify the correctness of the equivalent circuit network model. In order to solve the circuit network, the calculation method of the channel conductivity is described.

Physical model and computational method

In the present study, three ordered array configurations with mono-sized columns were investigated both by numerical simulation and network modelling. The studied cases include the in-line array, the staggered array and the hexagonal array. Physical models will be described in this section and the computational method in numerical simulation will be given.

Model description

The computational domains of three ordered array configurations studied are shown in fig. 1 and dimensions for each configuration are listed in tab. 1. Numerical simulations of the columns were carried out using ANSYS FLUENT R16.0 to provide the flow field in order to verify the correctness of the equivalent circuit network model. The flow in the computa-

tional domain is considered to be incompressible, steady, and laminar. The inlet is set as velocity inlet and the outlet is set as pressure outlet. Air is adopted as the working fluid having constant thermal properties. The SIMPLE algorithm is employed to couple the velocities and pressure. Second-order upwind scheme is used for the convective terms in the momentum equation. The residual of the calculation is less than 10^{-7}.
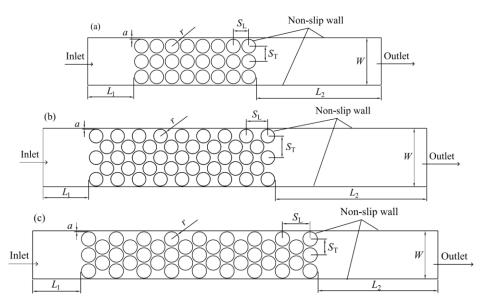
Figure 1. Different configurations; in-line array (a), staggered array (b), hexagonal array (c)

Table 1. Dimensions in different configurations

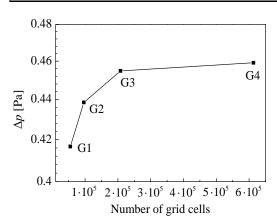| Configuration	L_1 [mm]	L_2 [mm]	W [mm]	A [mm]	S_L [mm]	S_T [mm]	R [mm]
In-line	30	100	31.00	1.00	10.00	10.00	4.50
Staggered	30	120	38.28	0.50	14.14	14.14	4.50
Hexagonal	30	120	30.00	0.50	17.32	10.00	4.50

Figure 2. Variation of pressure drop with number of grid cells

Grid independence test and model validation

The effect of the number of grid cells on the pressure drop was investigated. The variation of the total pressure drop in the in-line array with the number of grid cells is shown in fig. 2. Four grid systems are used. The difference of pressure drop between G3 and G4 is less than 1.0%. Therefore G3 is adopted in the following study.

The numerical method was validated by using a similar geometry, as shown in fig. 3. In fig. 3, the up and down edges are set as symmetry boundaries while the column surfaces are set as non-slip boundary conditions.

1990

Wang, J., *et al*.: Numerical Simulation and Circuit Network Modelling…
THERMAL SCIENCE: Year 2018, Vol. 22, No. 5, pp. 1987-1998

The pressure drop of this validation model under an inlet velocity of 0.01 m/s is 0.032 Pa. Lee and Yang [18] has proposed a correlation to calculate the pressure drop in porous structure. The pressure drop obtained by their correlation for the present model is 0.03188 Pa. The small deviation between the numerical results and Lee and Yang's correlation indicates the correctness of our numerical method.
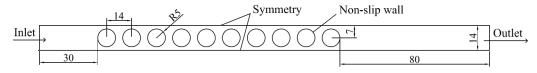

Figure 3. Geometry for model validation

Principle and method of network modelling

The flow in the packing configuration can be compared to the electric current in a circuit network. Therefore, the flow pattern in a certain packing configuration could be predicted by a circuit network instead of numerical simulation. In this section, how the circuit network is built and solved is given in details.

Network topology and geometry

From the numerical results of dense array configurations, we find the flow directions are similar to the array's Voronoi tessellation. The Voronoi cell (or Voronoi polygon) of a particle is delimited by the smallest envelope of bisecting lines with the other particles. The tessellation is unique. Each cell is convex and contains only one particle. The cell contains all those points closer to the given center than to any other, and hence a network of such polygons completely fills the space. Two particles whose cells have a common line are neighbors. The Voronoi tessellation in 2-D case is also called Thiessen polygon. In the present paper, the Thiessen polygon of a given array is obtained by MATLAB code. The Voronoi tessellations for each case are shown in fig. 4.
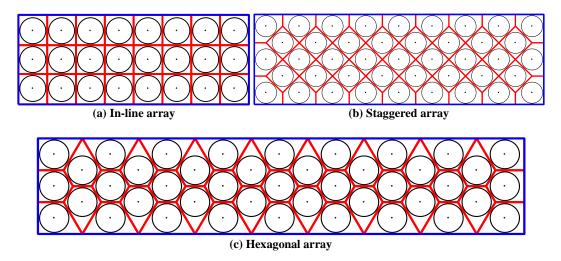

(a) In-line array **(b) Staggered array**

(c) Hexagonal array

Figure 4. Voronoi tessellations of different arrays

Electrical-fluidic analogy

The fluid-flow path in the array is closely related to the network of Voronoi polygon. In the network of Voronoi polygon, the vertex of each cell is regarded as the *node* in the flow circuit and the edge can be seen as the flow channel with a resistance. The analogy between electrical and mechanical (including fluidic) systems has been widely used. For a flow through the packed bed, the pressure drop, Δp, across the bed and the volumetric flow rate, Q, in the bed has the following relationship:

$$\Delta p = R_{hyd} Q \tag{1}$$

where the proportionality factor R_{hyd} is the hydraulic resistance. The relationship described in eq. (1) is completely analogous to Ohm's law given by:

$$\Delta V = RI \tag{2}$$

which relates the electrical current, I, through a wire with the electrical resistance, R, of the wire, and the electrical potential drop, ΔV, across the wire.

By using this analogy, it is possible to draw the equivalent electric circuit for a given array of particles, where the volumetric flow rate, Q, becomes the currents, the hydraulic resistances, R_{hyd}, in each channel becomes the resistors and pumps providing the pressure differences, Δp, becomes voltage sources (or current sources) [19].

Determination of hydraulic resistance

In eq. (1), if the hydraulic resistances of all channels are constant, then the resulting system of the electric equations is linear which is easy to slove. Otherwise, the circuit system is nonlinear and could be solved by Hardy-Cross method [20] or fixed-point iteration method [21].

In the present paper, we just consider the linear circuit system. Due to the complexity of the array configurations, only Darcy flow could guarantee a linear circuit system, where the pressure drop is proportional to the flow rate. In this case, the hydraulic resistance in each channel is just dependent to the geometry and is independent of the local velocity. For Darcy flow, the momentum equation has the following expression:

$$\nabla^2 \vec{u} = \frac{1}{\mu} \nabla p \tag{3}$$

where μ refers to the dynamic viscosity of the fluid, $\vec{u}$ – the velocity vector, and p – the pressure.

We find from eq. (3) that the equation for Darcy flow has the same expression as that of the Poiseuille flow. Therefore, the analytical solution could be adopted here. The relation between pressure drop, Δp, and the volumetric flow rate, Q, in 2-D Poiseuille flow is described:

$$\Delta p = \frac{12\mu L}{h^3} Q \tag{4}$$

where L is the length of the channel and h – the height between two plates.
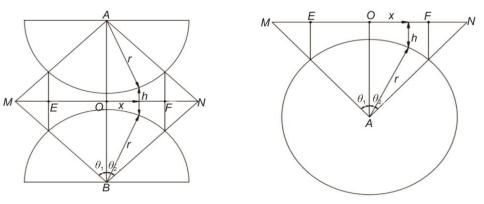
In the present study, the flow between two particles could be regarded as flow between two plates. However, different from the standard Poiseuille flow, the height between these two plates varies. Then the analytical solution for Poiseuille flow with changing height along the flow direction could be used here. According to [22], the relation between the pressure drop and the flow rate becomes:

$$\Delta p = 12\mu \int_0^L \frac{1}{h(x)^3} \, dx \, Q \tag{5}$$

Compared with eq. (1), the hydraulic resistance of the channel between two columns is calculated:

$$R_{hyd} = 12\mu \int_0^L \frac{1}{h(x)^3} \, dx \tag{6}$$

In the following text, we will describe how eq. (6) is used to calculate the hydraulic resistance for a certain channel. The channels in the studied cases could be divided into two types, one is the channel between two cylinder columns and the other is the one between the wall and the cylinder column. These two channels are shown in figs. 5(a) and 5(b), respectively.

(a) Channel between two columns   **(b) Channel between the column and the wall**

Figure 5. Sketch of the channels

As shown in fig. 5(a), the whole channel between two cylinder columns is from point *M* to point *N*. However, there is hardly pressure drop in the section of *ME* and *FN* where it corresponds to the pore. The pressure drop actually happens from point *E* to *F* where the flow is restricted by two column's surfaces. The height between two column's surfaces varies as the flow direction and has the following expression:

$$h = l_{AB} - 2\sqrt{r^2 - x^2} \tag{7}$$

where l_{AB} represents the distance between the center of two columns, r refers to the radius of columns, and x is the length along the flow direction calculated from point O where the rightward direction is positive. Substituting eq. (7) into eq. (6), the flow resistance between two columns is obtained by the following expression:

$$R_{hyd} = 12\mu \int_{-r\sin\theta_1}^{r\sin\theta_2} \frac{1}{h^3} \tag{8}$$

where θ_1 and θ_2 are the angles corresponding to the bounds of the integration.

As shown in fig. 5(b), the flow resistance in the channel between the wall and the column surface is similar with that between two columns. The difference is the height between the wall and the column surface which has the following expression:

Wang, J., *et al.*: Numerical Simulation and Circuit Network Modelling…
THERMAL SCIENCE: Year 2018, Vol. 22, No. 5, pp. 1987-1998

1993

$$h = l_{AO} - \sqrt{r^2 - x^2} \tag{9}$$

where l_{AO} represents the distance between the wall and the column surface.

Solving method of equivalent circuit model

After the flow network was confirmed and the flow resistance of each branch is determined, an equivalent circuit model was built by SIMULINK R2017b, a graphical extension to MATLAB for modelling and simulation of systems. Take the staggered array for example, its equivalent circuit diagram is shown in fig. 6. In fig. 6, the circuit is controlled by constant current source which represents the steady flow rate in the fluid-flow model. Each sub-circuit corresponds to one edge of the Voronoi polygon and contains a resistor which represents the hydraulic resistance. The current through each branch and the voltage of the branch are obtained by the current measurement and the voltage measurement, which can be displayed in the frame directly.
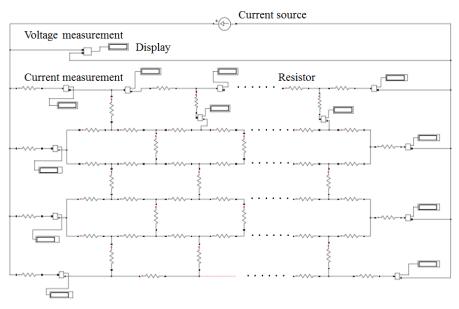

Figure 6. Equivalent circuit diagram of staggered array

Results and discussion

In this section, the flow regimes in three array configurations are studied by numerical study first, where the range of Darcy flow are determined since the present network model is only suitable for Darcy flow. Then the results of numerical simulation of network modelling for Darcy flow are compared to see whether the later one could predict the flow pattern with a high accuracy.

Flow regimes in array configurations

The flow regimes in porous media include Darcy, weak inertia, strong inertia, and turbulence as the velocity increases. In order to define the range of Darcy flow, the total pressure drops in three configurations under different inlet velocities were investigated by numer-

1994

Wang, J., *et al.*: Numerical Simulation and Circuit Network Modelling…
THERMAL SCIENCE: Year 2018, Vol. 22, No. 5, pp. 1987-1998

ical simulation. The results are shown in fig. 7. The curves of the total pressure drop *vs.* inlet velocity have similar trends in the three configurations we studied. When the inlet velocity is small, the total pressure drop is proportional to the inlet velocity where the flow proves to be Darcy flow (Region I). As the inlet velocity exceeds the critical value, the linear relationship between the pressure drop and the flow no longer exists where with the increase of the inlet velocity, the pressure drop increases more quickly (Region II).
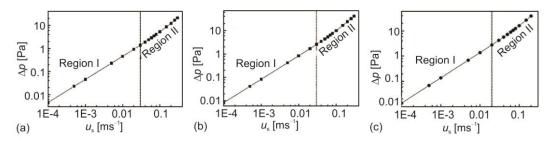

Figure 7. Variations of pressure drop with inlet velocity in different configurations: (a) in-line, (b) staggered, (c) hexagonal

For in-line array and staggered array, flow with inlet velocity smaller than 0.03 m/s could be regarded as Darcy flow while in the hexagonal array, Darcy flow is realized only when the inlet velocity is smaller than 0.02 m/s. Figure 8 depicts the local maximum velocities under each inlet velocity of these configurations. It could be found from fig. 8 that, though the critical inlet velocity of Darcy flow differs in three configurations, the critical value of local velocity for Darcy flow is almost the same, around 0.37 m/s. By defining the local Reynolds number as $\rho u d_{h}/\mu$, where the hydraulic diameter equals to two times of the height between two plates, it could be summarized that Darcy flow is achieved when the maximum Re_{local} is below 40.

From the previous results, it is found when inlet velocity is 0.01 m/s, the flow is in the range of Darcy flow, therefore, in the next section, we will adopt 0.01 m/s as the inlet velocity to study the effectiveness of the present network model.

Comparison of numerical simulation and network modelling for Darcy flow

Figure 9(a) shows the velocity contour of numerical results while fig. 9(b) shows the flow rate distribution of the network model in the in-line array configuration. From fig. 9(a) we could find that in the in-line array, fluid flows mainly in the
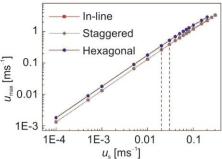

Figure 8. Local maximum velocities under each inlet velocity of three configurations

axial direction instead of the radial direction. There are four main flow channels including the channels between two columns and those between the column and the wall. The flow pattern in in-line array could be well represented by the equivalent circuit model, as shown in fig. 9(b). From the numerical results, it is easy to obtain the flow rate in each channel by integrating the velocity. The flow rates of the four main channels, from the top to the bottom, are $6.38 \cdot 10^{-5}$ m^3/s, $8.94 \cdot 10^{-5}$ m^3/s, $8.94 \cdot 10^{-5}$ m^3/s, and $6.39 \cdot 10^{-5}$ m^3/s, respectively. While the results predicted by the circuit network model are $6.64 \cdot 10^{-5}$ m^3/s, $8.88 \cdot 10^{-5}$ m^3/s, $8.88 \cdot 10^{-5}$ m^3/s,

and $6.64 \cdot 10^{-5}$ m^3/s. The maximum deviation is 4.08%. In additional, the total pressure drop of these two methods is compared. The pressure drop of numerical simulation is 0.4548 Pa while that of the network model is 0.4122 Pa. The deviation is −9.37%. For the in-line array configuration, we could find the present network could describe the flow pattern with a high accuracy.
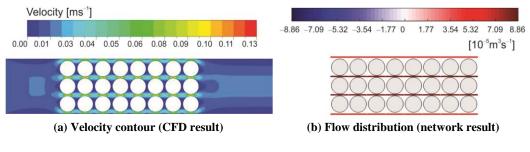

(a) Velocity contour (CFD result)   **(b) Flow distribution (network result)**

Figure 9. Fluid-flow in in-line array configuration
(*for color image see journal web site*)

From fig. 10, it could be seen that in the staggered array configuration, the flow pattern obtained by the numerical simulation and the network model are similar. The flow rate in the inner bed has the same value and is higher than that in the near wall region. We could find from fig. 10(a) that the flow path in the near wall region is a curve along the column surface, and it seems to be connected to the flow from the inner region. However, this characteristic cannot be caught by the equivalent circuit model. Instead, a vertical channel is used to connect the channels near the wall and in the inner. The vertical channel is predicted to have no flow rate, meaning that the fluid is not likely to flow from the top channel to the inner channel or in a diverse direction. This is the same case in the numerical result. Although there is some connection of flow in the vertical direction, no fluid is going to flow from the current channel to the other channel. Therefore, the network model is still a quick method to predict the flow pattern in the staggered array configuration with not so many details desired.
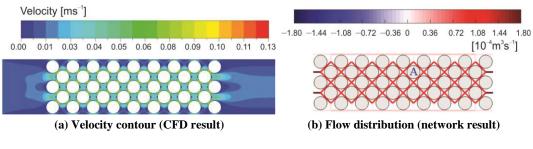

(a) Velocity contour (CFD result)   **(b) Flow distribution (network result)**

Figure 10. Fluid-flow in staggered array configuration
(*for color image see journal web site*)

Then the values obtained by the network model and numerical simulation are compared. The flow rates and pressure drops in the channels in the middle of the array, around particle A, shown in fig. 10(b), are shown in fig. 11. Here, we could see the deviation of the flow rate is all less than 5.98% while that of the pressure drop is within ±4.81%. From the results, it could be concluded that the circuit network is applicable for the staggered array configuration.

1996

Wang, J., *et al.*: Numerical Simulation and Circuit Network Modelling…
THERMAL SCIENCE: Year 2018, Vol. 22, No. 5, pp. 1987-1998

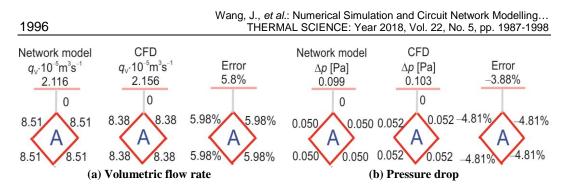(a) Volumetric flow rate   (b) Pressure drop

Figure 11. Comparison of numerical results and network results for staggered array

The velocity contour and flow distribution obtained by numerical simulation and network modelling in the hexagonal array are depicted in fig. 12. Here, it could be seen that the flow paths predicted by the network model is in accordance with the CFD result. The flow rates and pressure drops of channels surrounding particles A, B, and C, shown in fig. 12(b), by these two methods are illustrated in fig. 13. The maximum deviations of the flow rate and pressure drop are 8.43% and 5.71%, respectively. That indicates a good accuracy of the present network model.
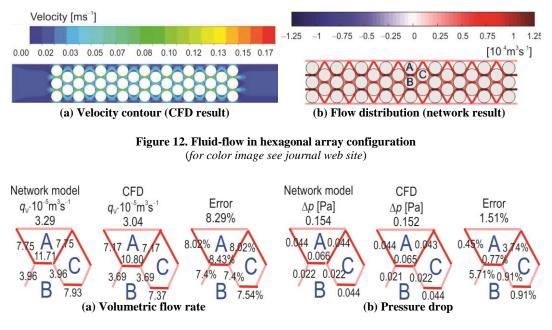

(a) Velocity contour (CFD result)   (b) Flow distribution (network result)

Figure 12. Fluid-flow in hexagonal array configuration
(*for color image see journal web site*)

(a) Volumetric flow rate   (b) Pressure drop

Figure 13. Comparison of numerical results and network results for hexagonal array

Conclusions

In the present paper, we performed the numerical simulation on three ordered array configurations to study the flow pattern in them. The flow regime of Darcy flow and non-Darcy flow is analyzed. An equivalent circuit model based on the Voronoi tessellation of the configuration is proposed to predict the flow distribution with the flow resistance being defined. Main conclusions are as follows.

- The demarcation point between Darcy flow and non-Darcy flow is dependent on the local Reynolds number instead of the inlet velocity. When the maximum local Reynolds number is below 40, the flow in the 2-D array configuration could be regarded as Darcy flow.
- In Darcy flow regime, the flow resistance in each channel of the configuration is a constant which could be determined by the analytical solution of Poiseuille flow with various cross-sections along the flow direction.
- The flow network in the array configuration could be described by an equivalent circuit model where the circuit network is built based on the Voronoi tessellation of the configuration. This model proves to be reliable to predict the flow distribution in ordered array configurations including in-line array, staggered array and hexagonal array in the range of Darcy flow.

Acknowledgment

Nomenclature

a – distance between the wall and particle column, [m]
d_h – hydraulic diameter, [m]
h – height between two plates, [m]
I – current, [A]
Q – volumetric flow rate, [m^3s^{-1}]
R – electric resistance, [Ω]
r – radius of particle column, [m]
R_{hyd} – hydraulic resistance, [m]
Re – Reynolds number ($= \rho u d_h/\mu$), [–]

S_L – longitudinal distance between 2 columns, [m]
S_T – transverse distance between 2 columns, [m]
u – velocity, [ms^{-1}]
W – width of the configuration, [m]

Greek symbols

ΔV – voltage drop, [V]
μ – dynamic visocity, [Pa s]
ρ – density, [kgm^{-3}]

References

[1] Yang, J., *et al.*, Experimental Analysis of Forced Convective Heat Transfer in Novel Structured Packed Beds of Particles, *Chemical Engineering Science*, *71* (2012), 6, pp. 126-137
[2] Li, L., *et al.*, Numerical Investigation on Band-Broadening Characteristics of an Ordered Packed Bed with Novel Particles, *Applied Energy*, *185* (2017), Part 2, pp. 2168-2180
[3] Arjun, K. S., Kumar, R., Optimization of Micro Pin-Fin Heat Sink with Staggered Arrangement, *Thermal Science*, On-line first, https://doi.org/10.2298/TSCI161221202A
[4] Sayehvand, H. O., *et al.*, Numerical Study of Forced Convection Heat Transfer over Three Cylinders in Staggered Arrangement Immersed in Porous Media, *Thermal Science*, *22* (2018), 1, pp. 467-475
[5] Wang, J. Y., *et al.*, Experimental and Numerical Study on Pressure Drop and Heat Transfer Performance of Grille-Sphere Composite Structured Packed Bed, *Applied Energy*, On-line first, https://doi.org/10.1016/j.apenergy.2017.07.140
[6] Hassan, Y. A., Dominguez-Ontiveros, E. E., Flow Visualization in a Pebble Bed Reactor Experiment Using PIV and Refractive Index Matching Techniques, *Nuclear Engineering & Design*, *238* (2008), 11, pp. 3080-3085
[7] Johns, M. L., *et al.*, Local Transitions in Flow Phenomena through Packed Beds Identified by MRI, *AIChE Journal*, *46* (2000), 11, pp. 2151-2161
[8] Marek, M., Numerical Simulation of a Gas Flow in a Real Geometry of Random Packed Bed of Raschig Rings, *Chemical Engineering Science*, *161* (2017), Apr., pp. 382-393
[9] Das, S., *et al.*, DNS Study of Flow and Heat Transfer through Slender Fixed-Bed Reactors Randomly Packed with Spherical Particles, *Chemical Engineering Science*, *160* (2017), Mar., pp. 1-19
[10] Yu, D., Numerical Simulation of Highly Dense Particle Packing under Vibration (in Chinese), Northeastern University, Shenyang, China, 2008.

[11] Oger, L., *et al.*, Voronoi Tessellation of Packings of Spheres: Topological Correlation and Statistics, *Philosophical Magazine B*, *74* (1996), 2, pp. 177-197
[12] Wu, H., *et al.*, Numerical Simulation of Heat Transfer in Packed Pebble Beds: CFD-DEM Coupled with Particle Thermal Radiation, *International Journal of Heat & Mass Transfer*, *110* (2017), July, pp. 393-405
[13] Chareyre, B., Cortis, A., Pore-Scale Modeling of Viscous Flow and Induced Forces in Dense Sphere Packings, *Transport in Porous Media*, *94* (2012), 2, pp. 595-615
[14] Koplik, J., Creeping Flow in Two-Dimensional Networks, *Journal of Fluid Mechanics*, *130* (1983), May, pp. 468-469
[15] Chu, C. F., Ng, K. M., Flow in Packed Tubes with a Small Tube to Particle Diameter Ratio, *AIChE Journal*, *35* (1989), 1, pp. 148-158
[16] Larachi, F., *et al.*, X-Ray Micro-Tomography and Pore Network Modeling of Single-Phase Fixed-Bed Reactors, *Chemical Engineering Journal*, *240* (2014), 6, pp. 290-306
[17] Hannaoui, R., *et al.*, Pore-Network Modeling of Trickle Bed Reactors: Pressure Drop Analysis, *Chemical Engineering Journal*, *262* (2015), Feb., pp. 334-343
[18] Lee, S. L., Yang, J. H., Modeling of Darcy-Forchheimer Drag for Fluid Flow across a Bank of Circular Cylinders, *International Journal of Heat & Mass Transfer*, *40* (1997), 13, pp. 3149-3155
[19] Mou, N., *et al.*, Coupled Equivalent Circuit Models for Fluid Flow and Heat Transfer in Large Connected Microchannel Networks – the Case of Oblique Fin Heat Exchangers, *International Journal of Heat and Mass Transfer*, *102* (2016), Nov., pp. 1056-1072
[20] Peter, I. C., Mann, R., A Network-of-Voids Model to Assess Wall Flow Patterns and Heat Transfer for Low Aspect Ratio Packed-Bed Reactors, *International Journal of Chemical Reactor Engineering*, *6* (2008), 1, pp. 77-90
[21] Lim, C. S., Ti, H. C., Mixed Specification Problems in Large-Scale Pipeline Networks, *Chemical Engineering Journal*, *71* (1998), 1, pp. 23-35
[22] Bruus, H., *Theoretical Microfluidics*, Oxford University Press, Oxford, UK, 2008